ELSEVIER

Il Farmaco 57 (2002) 469–478

IL FARMACO

www.elsevier.com/locate/farmac

Cytisine derivatives as high affinity nAChR ligands: synthesis and comparative molecular field analysis

O. Nicolotti [a], C. Canu Boido [b], F. Sparatore [b], A. Carotti [a,*]

[a] *Dipartimento Farmaco Chimico, Università degli Studi, via E. Orabona 4, I-70125 Bari, Italy*
[b] *Dipartimento di Scienze Farmaceutiche, Università degli Sudi, Viale Benedetto XV 3, I-16132 Genova, Italy*

Received 7 December 2001; accepted 16 February 2002

Abstract

A number of new N-substituted cytisine derivatives were prepared and tested, along with similar compounds already described by us and others, as high affinity neuronal acetylcholine receptor ligands. Structure–affinity relationships were discussed in the light of our recently proposed pharmacophore model for nicotinic receptor agonists. The most significant physicochemical interactions modulating the receptor–ligand binding were detected at the three dimensional (3D) level by means of comparative molecular field analysis (CoMFA). The best predictive PLS model was a single-field steric model showing good statistical figures: $n = 17$, $Q^2 = 0.717$, $s_{cv} = 0.566$, $r^2 = 0.942$, $s = 0.275$.

Keywords: N-substituted cytisines; Neuronal nicotine acetylcholine receptors; 3D QSAR; Scrambling

1. Introduction

Neuronal nicotinic acetylcholine receptors (nAChRs) are interesting targets for the development of novel drugs to treat a variety of CNS disorders [1,2], particularly Alzheimer's and Parkinson's diseases and opiate resistant chronic pain. Both agonists and antagonists could be of value in different pathologic conditions, though most efforts are presently directed at the discovery of highly subtype-selective agonists [3].

The need for selective agonists for central nAChR promoted the synthesis of a large number of structural analogues of nicotine and epibatidine [3,4], two very potent natural agonists. However, it is worth noting that both of them are endowed with many undesirable side effects. Particularly epibatidine, which is a very potent analgesic agent, is an extremely toxic compound, about 100 fold more toxic than nicotine in mice [5]. Thus nicotine and epibatidine may be questionable models for developing new drugs, though some success has been achieved with ABT-594 (a 2-chloro-5-pyridyl ether), which exhibited a quite improved therapeutic profile as an analgesic with respect to epibatidine [6,7].

Another important nicotinic agonist, which could disclose new perspectives and opportunities for developing new agonists and/or antagonists, is represented by cytisine, an alkaloid isolated from seeds of *Laburnum anagyroides*. In fact cytisine showed high affinity for many nAChR subtypes and is able to discriminate among some of them [8–10].

Though its pharmacological profile has been thoroughly studied [11–16], cytisine has not received much attention as a model for structural analogues or derivatives able to interact, directly or allosterically, with one or more receptor subtypes.

Main drawbacks of cytisine may depend on its low lipophilicity, which could hamper the crossing of the blood brain barrier, as shown by Reavill et al. [17] and also on its high affinity for α_3 containing (gangliar) subtypes, though lower than that for $\alpha_4\beta_2$ subtype. Recent studies have shown that an acetylcholine binding pocket is situated on each of the two α subunits of the pentameric nicotinic receptor, in a region at about 30 Å above the cell membrane. These pockets are connected to the water filled channel vestibule by narrow, 10–15 Å long, tunnels by which ACh might gain access to them [18,19]. However, on the basis of the crystal structure of the molluscan ACh-binding protein, the last possibility is considered unlikely by Brejc et al.

* Corresponding author.
E-mail address: carotti@farmchim.uniba.it (A. Carotti).

0014-827X/02/$ - see front matter
PII: S0014-827X(02)01216-8

[20]. These authors suppose that the most likely access routes to the ligand-binding sites are from above or below the double cysteine-containing loop C. These binding sites may be allosterically coupled with a non-competitive inhibitor (NCI) site, which is positioned within the central transmembrane domain of the ion channel, at the level of the extracellular surface of the bilayer, with a transverse distance from agonist sites in the range of 20–30 Å [21].

In the search for new nAChR subtype selective ligands, some of us have recently synthesized and characterized a number of cytisine derivatives [22,23], which have the secondary amine function substituted by residues that could modify the discriminating capability towards the nicotine receptor subtypes increasing also, in most cases, the lipophilicity of the parent compound. The size of the N-substituents and the additional chemical functionalities introduced with them may give rise to molecules which could still act as an agonist (even partial), or, extending outside the agonist volume, could act as competitive antagonist or yet by binding to the NCI site, as non-competitive antagonist.

We are herewith describing the preparation of additional N-substituted cytisine derivatives, which, together with part of previously prepared compounds, are assayed for nAChR affinity, through the displacement of [^{3}H]cytisine from rat brain membrane preparations. Results of these assays are to be considered with care, being the expression of the average affinity to the subtype population present in the receptor preparation, though the $\alpha_4\beta_2$ subtype is definitely prevailing.

Binding affinity data of cytisine derivatives **1**–**23**, listed in the Table 1, were analyzed by a three dimensional quantitative structure-activity relationships (3D QSAR) approach, that is the comparative molecular field analysis (CoMFA) [24] to derive predictive 3D QSAR models for this interesting, but almost unexplored class of nicotinic receptor ligands.

2. Chemistry

Most of the compounds object of the present study have been already described, either by us (**5**, **9**, **12**, **13**, **18**, **19** [22], **14**, **15**, **16** [23]) or by other authors (**2**, **3** [25], **17** [26,27], **21**, **22** [28]). The new compounds **4**, **6**–**8** and **10** were prepared by straight reactions between cytisine and the suitable halo compound. However, a thorough choice of solvents and reaction conditions was very important for a successful alkylation or acylation.

Compound **20**, as the previously described **18**, was obtained by reacting cytisine with the dihalo-compound in a 4:1 molar ratio; the use of other acid acceptors was not profitable. On the other hand, as already observed [22], compound **19** cannot be prepared in the same way, but required the preliminary formation of *N*-(3-chloropropyl)cytisine to be successively reacted with a second molecule of cytisine. Similarly, to obtain compound **23**, *N*-(4-chlorobutyn-1-yl)cytisine was firstly prepared and then reacted with pyrrolidine.

Compound **11** was formed by reacting cytisine with cyclohexylisothiocyanate.

Finally, nitrocytisine **21** was prepared, as described by Freund and Friedmann [28] by nitrating cytisine with 100% nitric acid and decomposing the formed *N*-nitrosonitrocytisine with ethanolic hydrogen chloride. The position of the nitro group was not defined by the German authors, which, however, considered nitrocytisine as a unitary compound.^{1}H NMR and ^{13}C NMR indicate that the obtained compound is a mixture of 3- and 5-nitrocytisine in a ratio of 3:1. Since this ratio is maintained in several preparations, the mixture was used as such in the binding assays.

Attempts for a complete separation of the two isomers are in progress.

The assignment of signals of NMR spectra to protons and carbon atoms of the pyridone ring of 3- and 5-nitrocytisine was rather easy since the signals are practically identical with those of 1-methyl-3-nitro- and 5-nitro-1H-pyridin-2-ones, respectively, [29,30] and, for the unsubstituted positions, with those of cytisine itself [31].

The UV absorption spectrum of the obtained nitrocytisines exhibits a maximum at 367 nm and a shoulder at 314 nm, which agree with the superimposition of spectra of 1-methyl-3-nitropyridin-2-one (λ_{max} 365 nm) and 1-methyl-5-nitropyridin-2-one (λ_{max} 305 nm) [29].

3. Experimental

3.1. Chemistry

Melting points (m.p.) were determined by the capillary method on a Büchi apparatus and are uncorrected.

Elemental analyses were performed with CE EA 1110 CHNS-O instrument and the results obtained for the indicated elements were within $\pm 0.4\%$ of the calculated values. UV and IR spectra were recorded, respectively, on Perkin–Elmer model 550S and Paragon 1000 PC spectrophotometers. ^{1}H and ^{13}C NMR were taken on a Varian Gemini 200 MHz spectrometer, using $CDCl_3$ or d_6-DMSO as solvent with TMS as internal standard.

3.1.1. *N*-Isopropylcytisine (**4**), *N*-allylcytisine (**6**), *N*-prenylcytisine (**7**)

A solution of cytisine (0.57 g, 3 mmol) in DMF (3 ml) was treated with 3.5 mmol of the suitable bromo-alkyl or alkenyl derivative and 0.4 ml of triethylamine.

The solution was heated at 140 °C in a sealed glass tube, for a time variable from 8 (allylderivative) to 48 h (isopropylderivative). After cooling, 3 ml of 2 N NaOH solution were added; triethylamine and part of the solvent were eliminated by heating under reduced pressure. The alkaline solution was extracted with dichloromethane obtaining an oil or a solid material which was worked up differently in the three cases.

N-Isopropylcytisine: the oil was chromatographed on alumina (10 g), eluting firstly with ether and then with ether plus 3% methanol. The viscous oil (0.2 g, 29% yield) was converted to the hydrochloride by a standard procedure; m.p. 264–268 °C (dec.).

Analysis (C, H, N) for $C_{14}H_{20}N_2O + 0.25H_2O$.

N-Allylcytisine: the solid was crystallized from ethanol–ether obtaining yellow crystals (120 mg, 18% yield) melting at 112–114 °C.

Analysis (C, H, N) for $C_{14}H_{18}N_2O$.

N-Prenylcytisine: the oil was rinsed several times with pentane leaving back some tarry material; from the pentane solution 0.3 g (39% yield) of an oil were obtained.

Table 1
Binding and physicochemical data of cytisine derivatives **1**–**23**

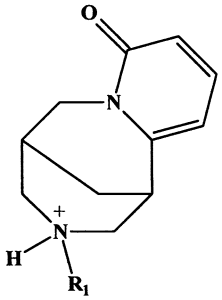

cmps	R_1	$pK_{i\ obs}$	pK_a [a]	ΔpKi_i [b]	ΔpK_i [c]
1	H (Cytisine)	8.62	11.22		-0.007
2	NH_2	8.44	8.19	0.09	0.305
3	N=O	7.41	3.87	-0.66	
4[d]	$CH(CH_3)_2$	5.64		-1.89	-0.689
5	$CH_2(CH_2)_3CH_3$	7.36			0.085
6[d]	CH_2-CH=CH_2	6.70		-0.92	-0.368
7[d]	CH_2-CH=$C(CH_3)_2$	6.92			0.002
8[d]	CH_2-C≡CH	7.00			0.069
9	$(CH_2)_2$-C(O)-CH_3	6.79			-0.038
10[d]	C(O)-OCH_2-CH_3	5.34	-1.20		
11[d]	C(S)-NH-C_6H_{11}	5.65	1.26		
12	CH_2-p-C_6H_4F	6.01			0.282
13	CH_2-CH=CH-C_6H_5	5.39		-0.32	0.232
14	2Cl-pyrid-6-yl	6.13		-0.81	0.364
15	2Cl-pyrazin-6-yl	6.10		-0.98	-0.052
16	3Cl-pyridazin-6-yl	5.32		-2.32	-0.301
17	H (3,5-dibromocytisine)	6.70		-0.62	
18	$(CH_2)_2$-(N12)Cytisine	7.02		0.06	-0.18
19	$(CH_2)_3$-(N12)Cytisine	7.52		0.03	-0.001
20[d]	$CH_2C{\equiv}CCH_2$-(N12)Cytisine	7.60		-0.11	0.133
21[e]	H (3/5-NO_2-Cytisine)	8.72		-0.41	
22	OH	6.37	5.51		
23[d]	$CH_2C{\equiv}CCH_2$-$N(CH_2)_4$	6.88		-0.29	0.165

(a) pKa values estimated by the LogDsol suite V5.0 software (ACD Toronto, Canada) on piperidine model system (b) Residual values (pKi observed – pKi predicted) calculated with a previously published CoMFA model[43]. (c) Residual values calculated from model S3 in Table 2. (d) New compounds. (e) Already described: now defined as a mixture of 3- and 5-nitrocytisine.

The oil was converted to the hydrochloride, that after crystallization from absolute ethanol–ether melted at 210–212 °C.

Analysis (C, H, N) for $C_{16}H_{22}N_2O + HCl + 0.5H_2O$.

3.1.2. N-Propargylcytisine ***(8)***

To a warm solution of cytisine (0.57 g, 3 mmol) in 15 ml of dry toluene, 0.36 g (3 mmol) of propargyl bromide and 0.4 ml of triethylamine were added; the solution was refluxed under nitrogen for 5 h. After cooling the precipitate was filtered and the solvent was removed under reduced pressure. The residue was treated with petroleum ether giving 0.42 g (60% yield) of crystals melting at 113–114 °C (dec.).

Analysis (C, H, N) for $C_{14}H_{16}N_2O + 0.25H_2O$.

3.1.3. 1,4-Bis(cytisin-12-yl)-2-butyne ***(20)***

To a solution of cytisine (0.76 g, 4 mmol) in warm acetonitrile (15 ml), a solution of 1,4-dichlorobutyne (0.1 ml, 1 mmol) in acetonitrile (1 ml) was dropped very slowly. The solution was refluxed under nitrogen for 2 h. After removing the precipitate and the solvent, the oily residue was partitioned between ether and acidic water. The acid solution was basified and extracted with dichloromethane, from which a solid residue was obtained. After crystallization from acetone–ether, the title compound (0.32 g, 81% yield) melted at 202–204 °C.

Analysis (C, H, N) for $C_{26}H_{30}N_4O_2 + 0.5H_2O$.

3.1.4. N-(4-Chloro-2-butyn-1-yl)cytisine

A solution of 1,4-dichlorobutyne (0.2 ml, 2 mmol) in acetonitrile (2 ml) was added to a solution of cytisine (0.76 g, 4 mmol) in warm acetonitrile (15 ml). The solution was refluxed under nitrogen for 4 h. The precipitate was filtered and the solvent was removed in vacuo. The residue was partitioned between ether and acidic water and the acid solution was basified and rapidly extracted with ether, which left 0.34 g (61% yield) of crystals melting at 114–116 °C.

Analysis (C, H, N) for $C_{15}H_{17}ClN_2O$.

3.1.5. 1-(Cytisin-12-yl)-4-(pyrrolidin-1-yl)-2-butyne ***(23)***

Pyrrolidine (0.1 ml, 1.2 mmol) was added, drop by drop, to a solution of *N*-(4-chloro-2-butyn-1-yl)cytisine (0.16 g, 0.6 mmol) in 10 ml of acetonitrile and the solution was refluxed under nitrogen for 4 h. The solvent was removed and the oily residue was rinsed several times with dry ether. The ether solution was evaporated obtaining 0.11 g (50% yield) of an oil.

Analysis (C, H, N) for $C_{19}H_{25}N_3O$.

The oil was converted to the hydrochloride that was crystallized from absolute ethanol–dry ether; m.p. > 250 °C.

3.1.6. N-(Ethoxycarbonyl)cytisine ***(10)***

Cytisine (0.57 g, 3 mmol) was dissolved in dry benzene (10 ml) and treated with freshly distilled ethyl chloroformate (0.3 ml, 3 mmol) and triethylamine (0.6 ml). The solution was refluxed under nitrogen for 5 h; after cooling the precipitate was filtered and the solvent removed under reduced pressure. The residue was distilled in a ball-tube at 0.1–0.05 Torr, raising the air bath temperature up to 190 °C. The distilled oil was rinsed with dry ether yielding 230 mg (29% yield) of crystals melting at 77–79 °C.

Analysis (C, H, N) for $C_{14}H_{18}N_2O_3$.

3.1.7. N-(Cyclohexylaminothiocarbonyl)cytisine ***(11)***

Cytisine (0.19 g, 1 mmol) was dissolved in absolute ethanol (8 ml) and treated with cyclohexylisothiocyanate (0.14 g, 1 mmol). The solution was heated at reflux for 3 h; after cooling the precipitate was collected and washed with cold ethanol and crystallized from the same solvent (0.25 g, 76% yield); m.p. 237–239 °C.

Analysis (C, H, N, S) for $C_{18}H_{25}N_3OS$.

3.1.8. N-Nitroso-3/5-nitrocytisine

To a suspension of cytisine (1.5 g, 7.8 mmol) in 1 ml of 65% nitric acid, 6 ml of 100% fuming nitric acid (degassed in vacuo) were added cautiously. The mixture was then heated at 110 °C for 20 min (until complete elimination of the vapors). The yellow solution was diluted with 15 ml of water and the precipitate was collected and washed thoroughly with water; a yellow powder (0.8 g) melting at 218–220 °C was obtained. The product was purified by dissolution in dimethylformamide and precipitation with ethanol; m.p. 237–244 °C. The German authors [28] used nitrobenzene instead of DMF.

Analysis (C, H, N) for $C_{11}H_{12}N_4O_4$.

3.1.9. 3/5-Nitrocytisine hydrochloride ***(21)***

N-Nitroso-3/5-nitrocytisine (0.2 g, 0.76 mmol) was treated with 4 ml of ethanol previously saturated with dry hydrogen chloride and the mixture was heated on a boiling water-bath. The product dissolved gradually, but another compound progressively precipitated. The heating was continued until a sample of the precipitate resulted completely soluble in water. After cooling the precipitate was filtered and washed with a little of ice-cold ethanol; pale yellow crystals with m.p. > 250 °C.

Analysis (C, H, N, Cl) for $C_{11}H_{13}N_3O_3 + HCl + 0.5H_2O$.

UV in EtOH: λ_{max} nm($\log \varepsilon$) = 367 (3.964); 314 sh (3.694); 265 sh (3.365).

^{1}H NMR (d_6-DMSO): 10.2 (s, 1H, exch. with D_2O); 9.0–8.5 (broad s, 1H exch. with D_2O); 8.44 (d, 0.75H, H-4 3-nitrocyt); 8.19 (d, 0.25H, H4 5-nitrocyt); 6.51 (d, 0.25H, H-3 5-nitrocyt); 6.48 (d, 0.75H, H-5 3-nitrocyt);

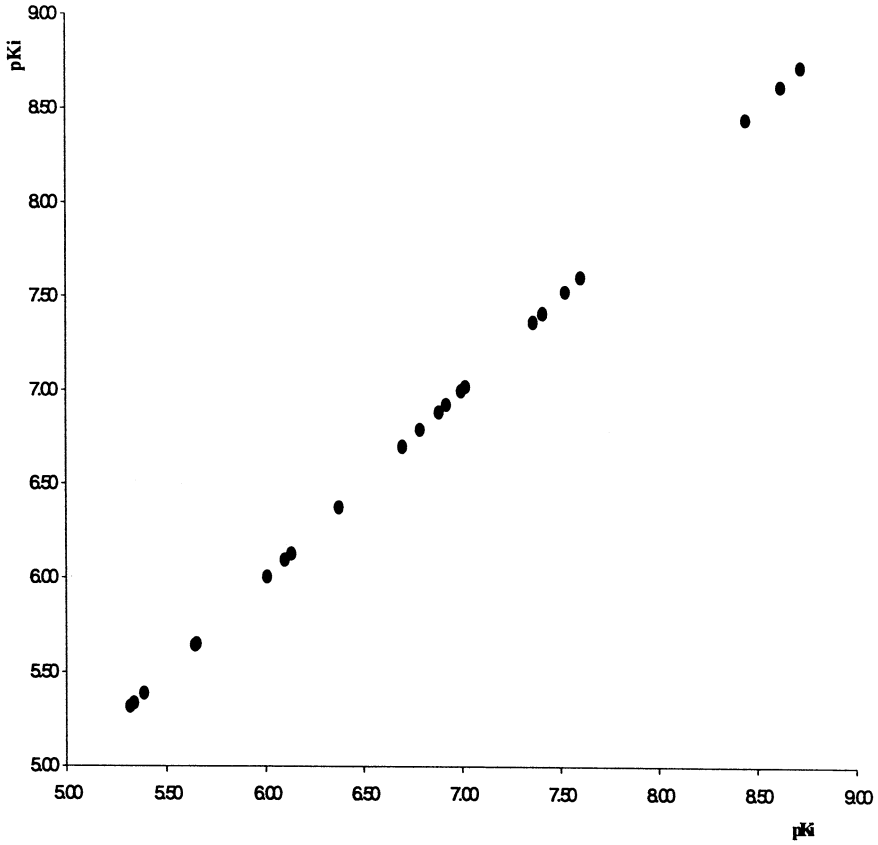

Fig. 1. Distribution of observed pK_i values.

4.30–3.80 (m, 2H); 3.70–3.00 (m, 5H); 2.70 (s, 1H); 2.20–1.80 (m, 2H).

^{13}C NMR (d_6-DMSO): 161.9 (CO, 5-nitrocyt); 156.7 (CO, 3-nitrocyt); 155.0 (C–NO_2, 3-nitrocyt); 138.15 (C-4, 3-nitrocyt); 135.7 (C-4, 5-nitrocyt); 131.1 (C–NO_2, 5-nitrocyt); 116.5 (C-3, 5-nitrocyt); 104.6 (C-5, 3-nitrocyt).

3.2. Receptor binding experiments

Binding assays were performed by MDS Panlabs Inc. (Bothell, WA, USA). Compounds were assayed either as hydrochlorides or as free bases, at four or five different concentrations in the range 10 μM–1 nM; each concentration was run in duplicate. The free bases were dissolved in DMSO at 10 mM concentration, and then diluted with water to 100 μM concentration.

Brain cerebral cortices were removed from Wistar rats and a membrane fraction was prepared by standard techniques, using 50 mM Tris–HCl buffer (pH 7.0 at room temperature, r.t.) containing 120 mM NaCl, 5 mM KCl, 1 mM $MgCl_2$ and 2.5 mM $CaCl_2$ [8]. Membrane preparation was incubated with [^{3}H]cytisine ($K_D = 3.2$ nM) at a concentration 2 nM for 75 min at 4 °C.

Non-specific binding was estimated in the presence of 100 μM nicotine.

Following incubation, the membranes were rapidly filtered under vacuum through glass fiber filters (Filtermats) and washed three times with ice cold buffer.

Bound radioactivity was measured with a scintillation counter (LKB Betaplate), using a scintillation fluid (Packard).

4. 3D QSAR study, results and discussion

Binding affinity data of cytisine derivatives **1**–**23**, listed in Table 1, are well suited for a QSAR study, spanning, quite regularly, a wide domain of activity (more than three orders of magnitude, see plot in Fig. 1: observed pK_i on both axes).

This is a good prerequisite for the derivation of reliable and statistically significant QSAR models. Unfortunately, the lack of physicochemical parameters for several substituents in our molecular set prevented the application of the classical QSAR approach (Hansch analysis) [32] that, for congeneric series, generally provides more reliable and easily interpretable models. For this reason the data set in Table 1 was analyzed by a 3D QSAR approach, that is the CoMFA.

CoMFA is a widely used tool for studying QSAR at the 3D level [33]. Unlike the conventional Hansch

analysis, which makes use of substituent parameters and multiple linear regression (MLR) to derive quantitative models, CoMFA considers as molecular descriptors the steric and electrostatic potentials, calculated within a grid surrounding the molecules, and partial least-squares (PLS) [34] as the regression method. CoMFA descriptors are, therefore, constituted by steric (Lennard–Jones) and electrostatic (Coulomb) potentials computed for each molecule, at each grid point, by means of a suitable probe, typically an sp^3 carbon atom with a charge of $+1$. PLS analysis produces model equations, which explain the variance in the biological activity in terms of the independent variables [35]. The optimum number of components (ONC, latent variables) is determined by cross validation (CV) and the model predictive ability is assessed by the CV correlation coefficient (r^2_{cv}, Q^2) [36]. The graphical representation of CoMFA results as isocontour maps allows an easy location of the regions where the variation in steric and electrostatic properties of the different molecules is correlated with the variation of biological activity.

Molecular models of cytisine derivatives in Table 1 were constructed from the fragment library of SYBYL 6.6 and their geometry optimized by the PM3 Hamiltonian within the suite of program MOPAC [37]. Each ligand molecule was subjected to a conformational analysis through a systematic search and the minimum energy conformers were selected for the superposition.

The molecular alignment is the most critical step in a CoMFA study [38]. In the present work, dealing with congeneric compounds, the molecular overlay was simply performed by choosing the rigid tricyclic skeleton of cytisine as the common anchor moiety.

Binding data in Table 1, were submitted to PLS analysis in conjunction with CV (leave-one-out method [39]) to derive the optimal number of components (ONC) to be used in the subsequent PLS analysis with a number of CV groups set to zero. However, in following strictly this procedure there is a risk of obtaining overfitted models due to a relatively high number of components to be used [40]. We, therefore, chose, from a plot of the squared CV coefficient Q^2 versus ONC, the first maximum in the curve. The selection of a lower number of components than ONC given by default in SYBYL yields poorer statistics in terms of r^2 and standard deviation (SD) (worse fitting), but more realistic and trustworthy models [41].

A preliminary analysis of the chemical structures of the examined ligands was conducted looking at their compliance with the nAChR pharmacophore recently developed in our group [42]. More precisely, in our pharmacophore hypothesis, three key interaction sites are regarded as pivotal for high nAChR affinity of agonists, namely: (i) a positively charged nitrogen atom for ionic or hydrogen bond interactions; (ii) a lone pair of the pyridine nitrogen or a specific lone pair of a carbonyl oxygen, as hydrogen bond site; and (iii) a dummy atom indicating the center of mass of hydrophobic moieties generally constituted by aliphatic rings. As a result, compounds, which do not show these three pharmacophore features, can constitute suspect points when building 3D QSAR models even when endowed with some residual receptor affinity.

An intimate look at estimated pK_a values of selected model molecules (i.e. simple piperidine derivatives) showed that at least four of them (**3**, **10**, **11** and **22**) should not be ionized at the pH of the binding assay (7.00) and as a consequence they do not possess the essential pharmacophoric group, that is the protonated nitrogen. Therefore, those ligands should be eliminated when deriving a CoMFA model. Indeed the lack of the protonated center ranked such compounds next to the lower bound of the affinity range, as observed for neutral derivatives **10** ($pK_i = 5.34$) and **11** ($pK_i = 5.65$) and for the *N*-hydroxycytisine derivative (**22**) ($pK_i = 6.37$) that should exist only partially in the protonated form (3%). Despite the lack of the positively charged nitrogen atom, unexpectedly the *N*-nitroso derivative (**3**) discloses an affinity ($pK_i = 7.41$) higher than that of the three uncharged derivatives mentioned above. This could be due, at least in part, to the (prevailing?) amphiionic hybrid, which would locate a positive charge on the pharmacophore nitrogen, and the corresponding negative charge on the oxygen of the nitroso group. However, the surprisingly high affinity of **3** does deserve further investigations.

On the basis of the previous discussion, cytisine derivatives **10**, **11** and **22** were discarded from the CoMFA study. Before performing such a study on the set of the remaining cytisine derivatives (**1**–**9**, **12**–**21** and **23**), we wanted to challenge the predictive power of our recently published CoMFA model [43], coming from the study of a very large array (206 cmps) of structurally diverse nAChRs agonists, comprising six cytisine congeners. For this purpose, the set of cytisine congeners in Table 1, not included in the previous model, was used as a true external prediction set. Their experimental binding affinities were normalized with respect to a pK_i value of 9.55 reported by Anderson [44] for cytisine and used by us in the derivation of the previous CoMFA models [43].

The molecular overlay was performed in two steps: first, the cytisine derivatives were superimposed on their common rigid tricyclic skeleton and the resulting supermolecule was superimposed onto the set of the remaining ligands already aligned on the three key pharmacophore features. The binding affinities of the external set of cytisine derivatives was thus predicted by the one-field steric CoMFA model developed for nAChR ligands ($n = 206$, ONC = 6, $Q^2 = 0.748$, $s_{cv} = 0.769$, $r^2 = 0.847$, $s = 0.600$) [43]. As can be seen in the column headed as ΔpK_i in Table 1, despite a general

overprediction trend and with the exception of some weak ligands (**4** and **16**), the binding affinities of cytisine derivatives were satisfactorily well predicted by the model.

To gain a better understanding at the 3D level of the main interactions responsible for the cytisine binding to nAChRs, the 20 selected cytisine derivatives (**1**–**9**, **12**–**21** and **23**) were thus submitted to a classical CoMFA run.

In agreement with previous findings, PLS models with good statistics were derived by considering the steric field alone (models S1–S4 in Table 2). Model S1 was derived from the 20 selected nAChRs ligands whereas model (S2) was developed by excluding two derivatives (**17** and **21**), which are the only ones bearing substituents on the pyridone moiety. Model S2 displayed remarkably improved statistics over model S1 also when only two components were taken into account ($Q^2 = 0.597$, $s_{cv} = 0.650$).

Model S3 was derived leaving out the *N*-nitroso derivative (**3**) as it was a strong outlier. This result constitutes an indirect validation of our three-points interaction pharmacophore model and in fact the exclusion of the *N*-nitroso derivative afforded a better model, both in statistical and interpretative terms. Model S3 represents the most satisfying model among those derived herein. However, we decided to derive also model S4 by leaving out the three dimeric derivatives (**18**, **19**, and **20**), which have a definitely longer and, in a certain way, unique structures. As can be seen in Table 2, model S4 still conserves good statistical figures.

A deep attention was then devoted to a further data validation. In the present work, a first glimpse of S3 model robustness reveals that the experimental values are regularly distributed around their theoretical points as can be observed in Fig. 2.

However, investigating the variation of Q^2 arising from CV-PLS analysis is the more appropriate and effective way to evaluating the QSAR prediction power

Table 2
Statistical results of CoMFA study of cytisine derivatives

Model	*n*	NOC [a]	Q^2 [b]	s_{cv} [c]	r^2 [d]	*s* [e]	Fields
S1	20	2	0.511	0.729	0.789	0.479	ste
S2	18	3	0.652	0.611	0.903	0.323	ste
S3	17	3	0.717 (−0.019) [f]	0.566 (1.223) [f]	0.942	0.255	ste
S4	14	3	0.774	0.547	0.977	0.175	ste

n, is the number of ligands.
[a] Number of optimal components.
[b] Squared cross-validation correlation coefficient.
[c] SD of errors of predicted values.
[d] Squared correlation coefficient.
[e] *s* of errors of fitted values
[f] More optimistic values after data scrambling.

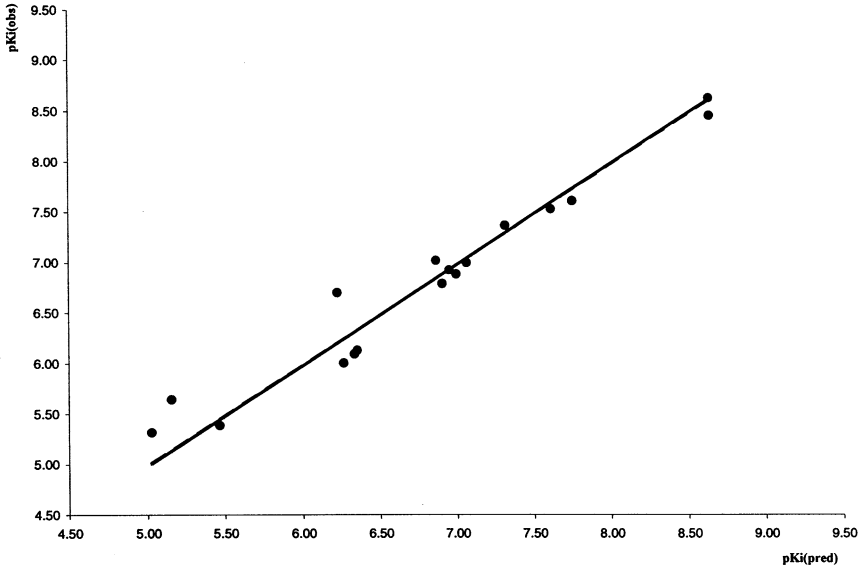

Fig. 2. Residual values distribution as calculated from model S3 in Table 2.

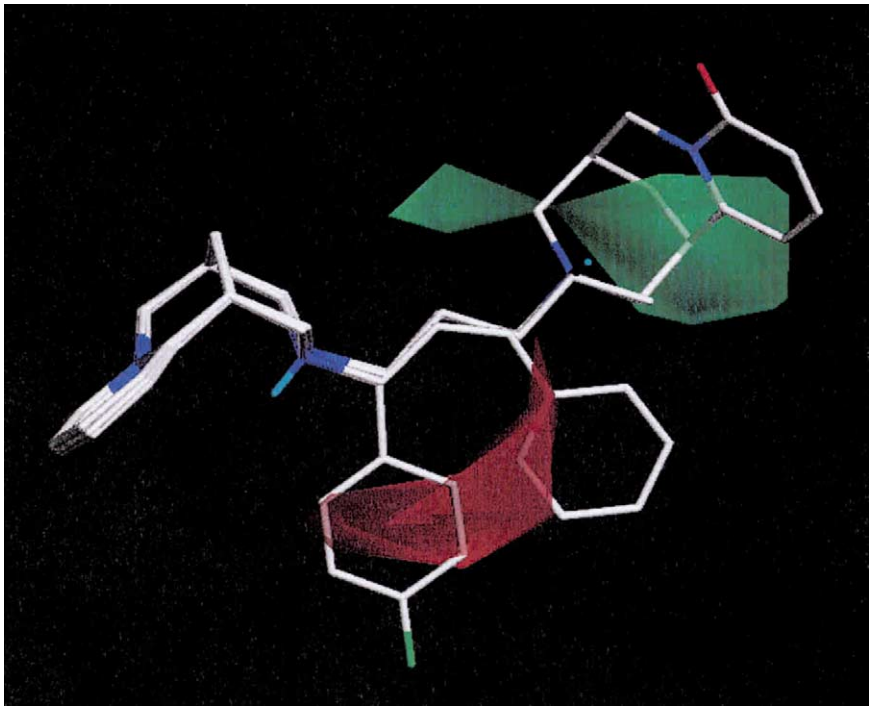

Fig. 3. Steric isocontour maps from steric model S3. Contour levels: red = −0.102, green = 0.020. Molecules shown to help interpretation have low (**12** and **13**) or high (**5** and **19**) binding affinity.

[39]. Concerning with the cytisines data set, the number of molecules is insufficient to perform the standard validation technique of CoMFA that is dividing the whole data set into a test set and a training set. Therefore, the affinity data randomization, better known as scrambling, was used as a procedure to validate the reliability of model S2. Basically, the biological activities (pK_i) were completely reassigned at random to the 17 compounds of models S3 and CV-PLS analyses were rerun. This procedure, repeated three times, always afforded low Q^2 and large s_{cv} values, as can be seen in Table 2 where the more optimistic Q^2 (the highest) and s_{cv} (the lowest) are reported.

The results from our 3D QSAR study offer a clear description of the possible receptor–ligand interactions over the whole substituent structural domain that spans from relatively small compound (**2**), up to the large-sized dimeric compounds (**18**–**20**), the latter conserving relatively high affinities.

Interestingly, the molecular branching of aliphatic substituents (compounds **4**–**7**) or the presence of relatively bulky aromatic–heteroaromatic moieties (compounds **12**–**16**), in the proximity of the charged nitrogen, plays a crucial role in ligand binding. These substituents may impact forbidden steric zones as can be easily seen in Fig. 3 for derivatives **12** and **13**.

On the other hand, compounds as the dimeric ligands **18**–**20**, which contains an even bulkier moiety but joined to the initial cytisine unit through a flexible straight carbon chain, show high pK_i values: the greater the length of the bridge, the higher the activity. Indeed, the steric isocontour maps of Fig. 3 suggest that they are able to reach sterically allowed regions (colored in green). The striking difference of activity of the dimeric ligands **18**–**20** compared with the *N*-cinnamyl derivative **13** (of similar overall molecular length) suggest the possibility that the second cytisine unit find some additional binding sites in the ACh binding pocket or in the preceding tunnel wall, not suitable to bind the phenyl ring of **13**.

The salient features of the CoMFA models indicated that steric and not electrostatic interactions modulated the ligand binding of cytisine to AChR. In fact, the PLS analysis of the electrostatic fields yielded no statistically significant models and moreover, even when the electrostatic field was combined with the steric one, a model worse than the single-field steric model was obtained (ONC = 3, $Q^2 = 0.550$, $s_{cv} = 0.705$). These findings are in full agreement with previous CoMFA models on nAChR agonists that showed a clear prevalence of steric over electrostatic interactions in the modulation of the ligand–receptor binding [43]. Indeed, steric maps in Fig. 3 contoured, at a more detailed level, the same spatial regions detected by the previous model [43].

Acknowledgements

Financial support by MURST and CNR (Rome) is gratefully acknowledged.

References

[1] C. Gotti, D. Fornasari, F. Clementi, Human neuronal nicotinic acetylcholine receptors, Prog. Neurobiol. 53 (1987) 199–237.
[2] F. Clementi, J. Court, E. Perry, D. Fornasari, Involvement of neuronal nicotinic receptor in disease, in: F. Clementi, D. Fornari, C. Gotti (Eds.), Neuronal Nicotinic Receptors, Handbook of Experimental Pharmacology, vol. 144, Springer, Berlin, 2000.
[3] G. Lloyd, M. Williams, Neuronal nicotinic receptors as novel drug targets, J. Pharmacol. Exp. Ther. 292 (2000) 461–467.
[4] M.W. Holladay, M.J. Dart, J.K. Lynch, Neuronal nicotinic acetylcholine receptor as targets for drug discovery, J. Med. Chem. 40 (1997) 4169–4194.
[5] J.P. Sullivan, M.W. Decker, J.D. Brioni, D.B. Donnelly-Roberts, D.J. Andersen, A.W. Bannon, C.-H. Kang, P. Adamas, M. Piattoni-Kaplan, M.J. Buckley, M. Gapalakrishnan, M. Willams, S.P. Arneric, Epibatidine elicits a diversity of in vitro and in vivo effects mediated by nicotinic acetylcholine receptors, J. Pharmacol. Exp. Ther. 271 (1994) 624–631.
[6] A.W. Bannon, M.W. Decker, M.W. Holladay, P. Curzon, D. Donnelly-Roberts, P.S. Puttfarcken, R.S. Bitner, R. Diaz, A.H. Dickenson, R.D. Porsolt, M. Williams, S.P. Arneric, Broad spectrum, non opioid analgesic activity by selective modulation of neuronal nicotinic acetilcholine receptors, Science 289 (1998) 77–81.
[7] M.W. Holladay, J.T. Wasicak, N.-H. Lin, Y. Ne, K.B. Ryther, A.W. Bannon, M.J. Buckley, D.J.B. Kim, M.W. Decker, D.J. Anderson, J.E. Campbell, T.A. Kuntzweirler, D.B. Donnelly-Roberts, M. Piattoni-Kaplan, C.A. Briggs, M. Williams, S.P. Arneric, Identification and initial structure-activity relationship of (R)-5-(2-azetidinylmethoxy)-2-chloropyridine (ABT 594), a potent, orally active non opiate analgesic agent acting via neuronal nicotinic acetylcholine receptors, J. Med. Chem. 41 (1998) 407–412.
[8] L.A. Pabreza, S. Dhawan, J.K. Kellar, [^{3}H]Cytisine binding to nicotine cholinergic receptors in brain, Mol. Pharmacol. 39 (1991) 9–12.
[9] M. Hall, L. Zerbe, S. Leonard, R. Freedman, Characterization of [^{3}H]cytisine binding to human brain membrane preparations, Brain Res. 600 (1993) 127–133.
[10] L.E. Chavez-Noriega, J.H. Crona, M.S. Washburn, A. Urrutia, K.J. Elliot, E.C. Johnson, Pharmacological characterization of recombinant and neuronal nicotinic acetylcholine receptors $h\alpha_2\beta_2$, $h\alpha_2\beta_4$, $h\alpha_3\beta_2$, $h\alpha_3\beta_4$, $h\alpha_4\beta_2$, $h\alpha_4\beta_3$, and $h\alpha_7$ expressed in *Xenopus oocytes*, J. Pharmacol. Exp. Ther. 280 (1997) 346–358.
[11] R.B. Barlow, L.J. McLeod, Some studies on cytisine and its methylated derivatives, Br. J. Pharmacol. 35 (1969) 161–174.
[12] J.W. Sloan, W.R. Martin, M. Bostwik, R. Hook, E. Wala, The comparative binding characteristics of nicotinic ligands and their pharmacology, Pharmacol. Biochem. Behav. 30 (1988) 255–267.
[13] E. Museo, R.A. Wise, Cytisine induced behavioural activation: delineation of neuroanatomical locus of action, Brain Res. 670 (1995) 257–263.
[14] T.S. Rao, L.D. Correa, R.T. Reid, G.K. Lloyd, Evaluation of antinocinoceptive effects of neuronal nicotinic acetylcholine receptors ligands in rat tail-flick assay, Neuropharmacology 35 (1996) 393–405.
[15] T.W. Seale, R.S. Singh, G. Basmadjan, Inherited selective hypoanalgesic response to cytisine in the tail-flick test in CF-1 mice, NeuroReport 9 (1998) 201–205.
[16] B. Ferger, C. Spratt, P. Teismann, G. Seitz, K. Kuschinsky, Effects of cytisine on hydroxyl radicals in vitro and MPTP-induced dopamine depletion in vivo, Eur. J. Pharmacol. 360 (1998) 155–163.
[17] C. Reavill, B. Walther, J.P. Stolerman, B. Testa, Behavioural and pharmacokinetic studies on nicotine, cytisine and lobeline, Neuropharmacology 29 (1990) 619–624.
[18] N. Unwin, Projection structure of the nicotinic acetylcholine receptor: distinct conformations of the α subunits, J. Mol. Biol. 257 (1996) 586–596.
[19] A. Miyazawa, Y. Fujiyoshi, M. Stowell, N. Unwin, Nicotinic acetylcholine receptor at 4.6 Å resolution: transverse tunnels in the channel wall, J. Mol. Biol. 288 (1999) 765–786.
[20] K. Brejc, W.J. van Dijk, R.V. Klaassen, M. Schuurmans, J. van der Oost, A.B. Smit, T.K. Sixma, Crystal structure of an ACh-binding protein reveals the ligand-binding domain of nicotinic receptors, Nature 411 (2001) 269–276.
[21] J.M. Herz, D.A. Johnson, P. Taylor, Distance between the agonist and non competitive inhibitor sites on the nicotinic acetylcholine receptor, J. Biol. Chem. 264 (1989) 12439–12448.
[22] C. Canu Boido, F. Sparatore, Synthesis and preliminary pharmacological evaluation of some cytisine derivatives, Farmaco 54 (1999) 438–451.
[23] E. Carbonelle, F. Sparatore, C. Canu Boido, R. Zwart, H.P.M. Vijverberg, F. Clementi, C. Gotti, Pharmacological and functional characterization of cytisine derivatives on rat neuronal nicotinic receptor subtypes, Br. J. Pharmacol., submitted for the publication.
[24] R.D. Cramer, D.E. Patterson, J.D. Bunce, Effect of shape on binding of steroid to carrier proteins, J. Am. Chem. Soc. 110 (1988) 5959–5967.
[25] G. Luputiu, F. Moll, *N*-Nitroso und *N*-Aminocytisin, Arch. Pharm. 306 (1973) 414–418.
[26] G. Luputiu, F. Moll, Die bromo-derivate des Cytisins, Arch. Pharm. 304 (1971) 151–158.
[27] P. Imming, P. Klaperski, M.T. Stubbs, G. Seitz, D. Gündish, Syntheses and evaluation of halogenated cytisine derivatives and of bioisosteric thiocytisine as potent and selective nAChR ligands, Eur. J. Med. Chem. 36 (2001) 375–388.
[28] M. Freund, A. Friedman, Zur Kenntnis des Cytisins, Chem. Ber. 34 (1901) 605–619.
[29] H. Möhrle, H. Weber, Substituenteneinfluss bei der Oxidation quartarer Pyrimidinium-verbindungen, Chem. Ber. 104 (1971) 1478–1489.
[30] G.B. Barlin, M.D. Fenn, A carbon-13 and proton nuclear magnetic resonance study of hydroxy and mercapto nitropyridines and their N-, O- and S-methyl derivatives and analogous compounds in dimethylsulfoxide, Heterocycles 24 (1986) 1301–1309.
[31] F. Bohlman, R. Zeisberg, ^{13}C NMR spectra of Lupinen-Alkaloiden, Chem. Ber. 108 (1975) 1043–1051.
[32] QSAR: Hansch analysis and related approaches, H. Kubinyi, Ed.; Escom: Leiden (1993).
[33] 3D QSAR in Drug Design: Theory, Methods and Applications, H. Kubinyi, Ed.; Escom: Leiden (1993).
[34] W.J. Dunn III, S. Wold, U. Edlund, S. Helberg, Multivariate structure–activity relationships between data from a battery of biological tests and an ensemble of structure descriptors: the PLS method, Quant. Struct. Act. Relat. 3 (1984) 131–137.
[35] S. Wold, E. Johansson, M. Cocchi, PLS—'Partial Least-Squares Projections to Latent Structures' in [33], pp. 523–549.
[36] R.D. Cramer III, J.D. Bunce, D.E. Patterson, Crossvalidation, bootstrapping and partial least-squares compared with multiple regression in conventional QSAR studies, Quant. Struct. Act. Relat. 7 (1988) 18–25.
[37] J.J.P. Stewart, MOPAC: a semiempirical molecular orbital program, J. Comput. Aided Mol. Des. 4 (1990) 1–103.

[38] R.D. Cramer, S.A. De Priest, D.E. Patterson, P. Hecht, The developing practice of CoMFA, in [33], pp. 443–485.
[39] S. Wold, L. Eriksson, Statistical validation of QSAR results, in: H. van de Waterbeemd (Ed.), Chemometric Methods in Molecular Design, VCH, Weinheim, 1996, pp. 309–318.
[40] G. Folkers, A. Merz, D. Rognan, CoMFA scope and limitations, in [33] pp. 583–618.
[41] S. Wold, PLS for multivariate linear modeling, in [39], 195–218.
[42] O. Nicolotti, M. Pellegrini-Calace, A. Carrieri, C. Altomare, N. Centeno, F. Sanz, A. Carotti, Neuronal nicotinic receptor agonists: a multi-approach development of the pharmacophore, J. Comput. Aided Mol. Des. 15 (2001) 859–872.
[43] O. Nicolotti, M. Pellegrini-Calace, C. Altomare, A. Carotti, F. Sanz, Ligands of neuronal nicotinic acetylcholine receptor (nAChR): inferences from the Hansch and 3-D quantitative structure–activity relationship (QSAR) models, Curr. Med. Chem. 9 (2002) 1–29.
[44] D.J. Anderson, S.P. Arneric, Nicotinic receptor binding of [^{3}H] cytisine, [^{3}H]nicotine and [^{3}H] methyl carbamylcholine in rat brain, Eur. J. Pharmacol. 253 (1994) 261–267.